Controlling magnetism of semi-magnetic quantum dots with odd-even exciton numbers

2008 EPL 81 37005

(http://iopscience.iop.org/0295-5075/81/3/37005)

A Letters Journal Exploring the Frontiers of Physics

February 2008

EPL, **81** (2008) 37005 www.epljournal.org
doi: 10.1209/0295-5075/81/37005

Controlling magnetism of semi-magnetic quantum dots with odd-even exciton numbers

S.-J. Cheng[1] and P. Hawrylak[2]

[1] *Department of Electrophysics, National Chiao Tung University - Hsinchu 300, Taiwan, Republic of China*
[2] *Institute for Microstructural Sciences, National Research Council - Ottawa, Canada*

received 11 August 2007; accepted in final form 29 November 2007
published online 7 January 2008

PACS 78.67.Hc – Quantum dots
PACS 75.75.+a – Magnetic properties of nanostructures
PACS 71.35.Gg – Exciton-mediated interactions

Abstract – We present a theory of optical control of magnetism in a self-assembled quantum dot (SAD) containing magnetic ions. We show that the magnetic state of Mn ions can be controlled by the number of excitons in the dot. For an odd number of excitons the magnetic ions are coupled by the spins of valence holes and electrons. For an even number of excitons we derive the effective RKKY interaction between Mn ions, and show that it is controlled by valence holes. We predict the emission spectra of the coupled Mn-exciton system and relate them to the magnetic state of ions and the number of excitons in the quantum dot.

Advances in magneto-electronics, from magnetic information storage, spintronics, to quantum information processing, rely on developing effective means of controlling magnetism other than an external magnetic field, and on creating distinct magnetic phases of magnetic medium allowing for reversible switching [1–4]. Several attempts have been made to use electric field, strain, and light for the engineering of magnetism [4–8]. In contrast to a variety of techniques developed for the control of magnetism, only few magnetic materials can exhibit distinct magnetic phases suitable for the encoding of bits of information [9]. Semi-conductor quantum dots [10] containing magnetic ions and a voltage-controlled number of electrons and/or valence holes offer means for the electrical control of magnetic properties [11–21]. Here we investigate means for the control of magnetic properties of magnetic ions via optical control of the average population of photo-excited electrons and holes [22–25].

Unlike in electronic quantum dots where orbital degeneracies lead to spin polarization following Hund's rules, in electron-hole quantum dots "hidden symmetries" guarantee that odd exciton numbers carry spin, and even exciton number complexes have no net spin [26,27]. We show that the odd exciton complexes form many-exciton-many-Mn polaron complexes where bright and dark excitons are mixed in a non-perturbative fashion. The even exciton complexes induce a RKKY-like interaction among magnetic ions [21]. The interaction is long ranged, is dominated by valence holes, and can be controlled on a time scale dominated by carrier generation and recombination times. This is similar to the work by Fernandez-Rossier and Brey [28] on electrons in quantum dots but different from the coherent control of the RKKY interaction of electronic spins in different dots via virtual electron-hole pair excitation proposed by Sham and co-workers [29,30].

The work presented here builds on experimental work on quantum dots with a single Mn ion by Mariette and co-workers [31,32] and theoretical work by Govorov [33] and Fernandez-Rossier and Brey [28,34]. We focus here on II–VI self-assembled quantum dots with few Mn ions as isoelectronic impurities. Following III–V quantum dots [27,35,36] the single-particle spectrum corresponding to a parabolic confining potential and a perpendicular magnetic field ($\vec{B} \parallel \vec{z}$) is a sum of two harmonic oscillators (HO): $\epsilon^{\beta}_{mn\sigma} = \Omega^{\beta}_{+}(n+1/2) + \Omega^{\beta}_{-}(m+1/2) + g_{\beta} u_B \vec{B} \cdot \vec{\sigma}$, where n, $m = 0,\ 1,\ 2\ldots$, $\sigma = \uparrow / \downarrow$ represents the spin $\vec{s}$ ($s_z = \pm 1/2$) for the electron, and $\vec{j}$ ($j_z = \pm 3/2$) for the heavy hole. The energies $\Omega^{\beta}_{+/-}$ are defined as $\Omega^{\beta}_{+/-} = \frac{1}{2}(\sqrt{\omega^2_{c,\beta} + 4\omega^2_{\beta}} \pm \omega_{c,\beta})$, where $\omega_{c,\beta} = eB/m^*_{\beta}$ is the cyclotron energy, m^*_{β} is the effective mass, and ω_{β} is the level spacing for particle β (either electron or a hole). The Bohr magneton is u_B and $g_{e/h}$ is the g-factor for the electron/hole. The energy spectrum of electrons in a d-shell of a single Mn ion is approximated here by a spectrum of a single angular momentum M with $M = 5/2$, and six states $|M_z\rangle$, with $M_z = -5/2, -3/2, -1/2, +1/2, +3/2, +5/2$.

Let us describe the Hamiltonian of many Mn ions coupled to electrons and valence holes. The magnetic ions interact with each other via the anti-ferromagnetic, short-ranged interaction $|J_{IJ}^{MM}|\vec{M}_I \cdot \vec{M}_J$ [2]. Each Mn ion at position $\vec{R}_I$ is coupled with the electron spin at $\vec{r}_e$ via the contact ferromagnetic exchange interaction $H_{eM} = -|J_{eM}^{2D}|\vec{s}\cdot\vec{M}_i\delta(\vec{r}_e - \vec{R}_i)$. The exchange interaction of the Mn ion with the valence hole $H_{hM} = +|J_{hM}^{2D}|\vec{j}\cdot\vec{M}_i\delta(\vec{r}_h - \vec{R}_i)$ is anti-ferromagnetic, with coupling strength significantly higher than that of the e-Mn interaction. The electron and hole spins are coupled via the exchange Coulomb interaction.

With M^+, M^- as Mn raising and lowering angular-momentum operators, and with the operators $c_i^\dagger$ ($h_i^\dagger$) and c_i (h_i) as the electron (hole) creation and annihilation operators, where i is a composite index of HO states $|i\rangle = |m,n\rangle$, the Hamiltonian of an interacting electron-hole-Mn system in the language of second-quantization reads

$$
\begin{aligned}
H \;=\; & \sum_I g_{Mn}u_B B M_I^z + \sum_{IJ}\frac{J_{IJ}^{MM}}{2}\vec{M}_I\cdot\vec{M}_J \\
& - \sum_{ijI}\frac{|J_{ij}^{eM}(\vec{R}_I)|}{2} \\
& \times [(c_{i\uparrow}^\dagger c_{j\uparrow} - c_{i\downarrow}^\dagger c_{j\downarrow})M_I^z + c_{i\downarrow}^\dagger c_{j\uparrow}M_I^+ + c_{i\uparrow}^\dagger c_{j\downarrow}M_I^-] \\
& + \sum_{ijI}\frac{|J_{ij}^{hM}(\vec{R}_I)|}{2}[(h_{i\uparrow}^\dagger h_{j\uparrow} - h_{i\downarrow}^\dagger h_{j\downarrow})M_I^z] \\
& + \sum_{ij}\sum_{\sigma_1^e,\sigma_2^e,\sigma_1^h,\sigma_2^h}\langle\sigma_1^e,\sigma_1^h|H_x^{ij}|\sigma_2^e,\sigma_2^h\rangle c_{i\sigma_1^e}^\dagger h_{j\sigma_1^h}^\dagger h_{j\sigma_2^h}c_{j\sigma_2^e} \\
& + \sum_i^\sigma \epsilon_{i\sigma}^e c_{i\sigma}^\dagger c_i + \sum_i^\sigma \epsilon_{i\sigma}^h h_{i\sigma}^\dagger h_{i\sigma} - \sum_{ijkl}^{\sigma,\sigma'} V_{ijkl}^{eh}c_{i\sigma}^\dagger h_{j\sigma'}^\dagger h_{k\sigma'}c_{l\sigma} \\
& + \frac{1}{2}\sum_{ijkl}^{\sigma,\sigma'} V_{ijkl}^{ee}c_{i\sigma}^\dagger c_{j\sigma'}^\dagger c_{k\sigma'}c_{l\sigma} + \frac{1}{2}\sum_{ijkl}^{\sigma,\sigma'} V_{ijkl}^{hh}h_{i\sigma}^\dagger h_{j\sigma'}^\dagger h_{k\sigma'}h_{l\sigma}.
\end{aligned}
\tag{1}
$$

The first two terms of the RHS of eq. (1) describe the Hamiltonian of Mn's, including the single Mn Zeeman energies ($g_{Mn} = 2.0$) and Mn-Mn interactions. The Mn subsystem is coupled to the electrons and holes. In the electron-Mn (the third term, second and third lines) and hole-Mn (the fourth line) interactions, the z-components of exciton spins act as an effective field acting on Mn spins. The last two terms in the electron-Mn interaction correspond to the electron spin flip scattering, compensated by Mn spin flips. By contrast, due to the spin-orbit coupling the hole spin is frozen along the growth direction (z-axis), and the hole-Mn interaction is of the Ising form [15]. The Ising-like form of the hole-Mn interaction is based on the fact that the hole spin in quasi-2D systems, such as quantum wells and self-assembled quantum dots, is frozen in the growth direction [37]. The e-Mn/h-Mn interaction strength $J_{ij}^{eM/hM}(\vec{R}_I) \equiv J_{eM/hM}^{2D}[\psi_i^{e/h}(\vec{R}_I)]^*\psi_j^{e/h}(\vec{R}_I)$ is determined by the wave function of the electron/hole at the position R_I of the I-th Mn. The fifth term of the RHS of eq. (1) describes the e-h spin-spin exchange interactions, while the last five terms of the RHS of eq. (1) contain kinetic energies, e-e, h-h, and e-h Coulomb interactions, where $V_{ijkl}^{\beta\beta'} \equiv \int\int \mathrm{d}\vec{r}_1\mathrm{d}\vec{r}_2\psi_i^{\beta *}(\vec{r}_1)\psi_j^{\beta' *}(\vec{r}_2)\times\frac{e^2}{4\pi\kappa|\vec{r}_1-\vec{r}_2|}\psi_k^{\beta'}(\vec{r}_2)\psi_l^{\beta}(\vec{r}_1)$, with $\kappa = 10.6\epsilon_0$ the dielectric constant.

The matrix elements for the e-h exchange interaction $\langle\sigma_1^e,\sigma_1^h|H_x^{ij}|\sigma_2^e,\sigma_2^h\rangle$ can be written in the basis of two bright $h_{j\uparrow}^\dagger c_{j\downarrow}^\dagger|vac\rangle$, $h_{j\downarrow}^\dagger c_{i\uparrow}^\dagger|vac\rangle$, and two dark $h_{j\uparrow}^\dagger c_{i\uparrow}^\dagger|vac\rangle$, $h_{j\downarrow}^\dagger c_{i\downarrow}^\dagger|vac\rangle$ states. They have been parametrized in *e.g.* ref. [38].

We now proceed to construct many-particle configurations of the Mn electron and hole system. We label the multi-exciton state by the number of excitons N_x, their total angular momentum L_{tot}, and the z-components of the total spin of electrons S_z^e and holes S_z^h *i.e.* $|N_x; L_{tot}; S_z^e; S_z^h\rangle$. We label the multi-Mn configurations by the number of Mn ions N_M and the z-component of the spin of each Mn, *i.e.* $|N_M; M_z^1 M_z^2 \ldots M_z^{N_M}\rangle$. The states of the coupled system are written as a linear combination of the exciton and Mn subsystems: $|N_x; N_M; i\rangle = \sum_{k=1}^{N_c} A_k^i|N_x; L_{tot}; S_z^e; S_z^h\rangle|N_M; M_z^1 M_z^2 \ldots M_z^{N_M}\rangle$. The energy spectrum is calculated by selecting a number N_s of lowest-energy single-particle states, constructing all possible electron-hole-Mn configurations N_c, corresponding to the total angular momentum L_{tot}, the z-components of the spins for electron, hole, and Mn ions, and constructing the Hamiltonian matrix. The eigenstates and eigenvalues in a space of N_c configurations are obtained by numerical diagonalization of the Hamiltonian matrix using the conjugated gradient algorithm. The numerical results are used to support analytical results given whenever possible.

To illustrate the general theory, to make contact with experiment, and to demonstrate how one can optically control magnetic interactions we focus on the simplest case of two interacting Mn ions positioned at $\vec{R}_1$ and $\vec{R}_2$, equally coupled to exciton carriers ($|\vec{R}_1| = |\vec{R}_2|$), in a SAD. We analyze in detail the magnetic state of Mn ions when the quantum dot is filled by either a single exciton (X) (odd exciton number), or by a bi-exciton (XX) (even exciton number). The effect of different Mn ion positions on the emission spectrum is discussed in ref. [34].

To emphasize the physics we limit the single-exciton state to four spin configurations $h_{(0,0)j_z}^\dagger c_{(0,0)s_z}^\dagger|vac\rangle = |s_z, j_z\rangle$. This is a good approximation for strongly confined dots. It allows us to to derive the more familiar effective spin Hamiltonian for an exciton coupled to two Mn ions: $H_{X2Mn} = |J_{12}^{MM}|\vec{M}_1\cdot\vec{M}_2 - \frac{2}{3}|\Delta_0|s_z\cdot j_z + |\bar{J}_{hM}|j_z M_z - |\bar{J}_{eM}|\vec{s}\cdot\vec{M}$, where $\vec{M} = \vec{M}_1 + \vec{M}_2$, Δ_0 is the splitting of the dark and bright exciton states resulting from the short-range e-h exchange interaction, and

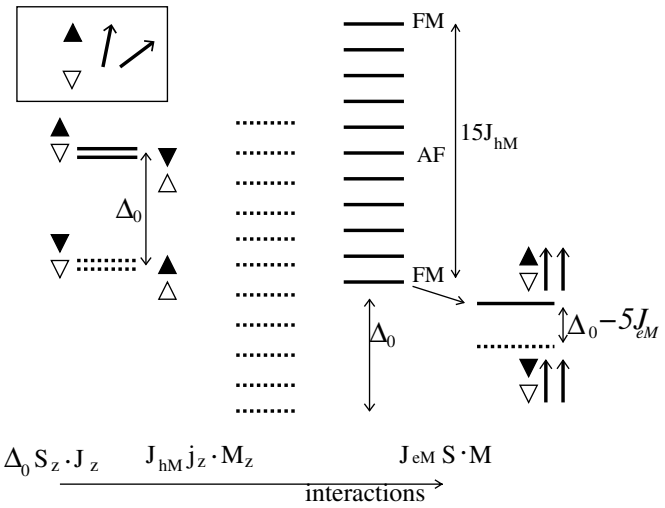

Fig. 1: Schematic diagram of energy shells of two Mn ions coupled to a single exciton. Filled (empty) triangles represent spin-down or spin-up electrons (holes) and solid arrows indicate Mn spins. Solid lines indicate optically active exciton states with $l = \pm 1$ and broken lines indicate dark exciton states with $l = \pm 2$.

$J_{eM/hM}(R_1) = J_{eM/hM}(R_2) \equiv \bar{J}_{eM/hM}$ is assumed. Here we neglect the long-range e-h interaction between bright excitons Δ_1 and the one between dark excitons Δ_2, which originate from the symmetry breaking of the dot shape and the intermixing of the light hole and heavy hole, respectively, and are known to be weak for symmetric strained SADs [38]. For brevity, the spin irrelevant kinetic energies and the e-h interaction of the exciton are not shown. The numerical results presented below are based on the spin Hamiltonian derived above from the general Hamiltonian eq. (1).

Figure 1 shows the schematic energy spectrum of two Mn spins coupled to a single X. Without the interactions with X, the 2Mn ions are in one of the nearly degenerate states $|M_z^1 M_z^2\rangle$, while the exciton states form dark ($l \equiv s_z + j_z = \pm 2$) and bright ($l = \pm 1$) doublets separated by the short-ranged e-h exchange energy Δ_0. When the hole-Mn interaction $|\bar{J}_{hM}| j_z M_z$ is turned on, each of the dark and bright doublets splits the degenerate Mn states into $2M + 1 = 11$ shells, spaced by $\frac{3}{2}|J_{hM}|$, corresponding to 11 possible values of total $M_z = -5, -4, \ldots, +4, +5$. The Mn shells coupled to the dark (bright) exciton are shown with broken (solid) lines in fig. 1. The lowest- and highest-energy shells correspond to the two fully polarized (FM) Mn ions with $M_z = \pm 5$, while the shell in the middle of the spectrum corresponds to the spin unpolarized (AF) Mn's with $M_z = 0$. The 11 levels span the energy range $15|J_{hM}|$ and the ground state corresponds to the ferromagnetic arrangement of Mn spins. We now turn on the electron-Mn interaction. The e-Mn interaction intermixes the bright and dark X spin states by simultaneously flipping electron and Mn spin, and makes the dark state optically active. The energy separation between the dark 1X ground state (GS) and the lowest bright state is reduced by the e-Mn interaction to $\Delta_0 - M|J_{eM}| = \Delta_0 - 5|J_{eM}|$, result obtained by retaining only the Ising part in the Hamiltonian. Hence, the odd number of excitons couples ferromagnetically the two magnetic ions, forming an excitonic magnetic polaron. In turn, magnetic ions change the optical properties of quantum dots by making dark exciton states optically active.

Let us now examine what happens when an additional exciton is injected into a quantum dot. Because of the singlet state of the bi-exciton, $h^\dagger_{(0,0)\uparrow} h^\dagger_{(0,0)\downarrow} c^\dagger_{(0,0)\downarrow} \times c^\dagger_{(0,0)\uparrow}|vac\rangle$ there is no direct coupling of electron and hole spins to magnetic ions [15,32]. The effective spin Hamiltonian for two Mn ions coupled to the spin singlet XX reduces to $H_{XX\text{-}2Mn} = +|J_{12}^{MM}|\vec{M}_1 \cdot \vec{M}_2$. However, the presence of electrons and holes leads to an effective RKKY interaction of Mn ions. Treating the e-Mn and h-Mn interactions as perturbations we evaluate in the second-order perturbation theory the shift in the GS energy, $\Delta E = \sum_k |\langle G|H_{eM} + H_{hM}|k\rangle|^2/(E_G - E_k)$, where $|G\rangle$ is the lowest XX-2Mn configuration and $|k\rangle$ are the excited XX-2Mn configurations based on the s- and p-shell states of a SAD. After some algebra, we obtain $\Delta\hat{E} = J_e^{RKKY}(\vec{R}_1, \vec{R}_2)\vec{M}_1 \cdot \vec{M}_2 + J_h^{RKKY}(\vec{R}_1, \vec{R}_2) M_1^z M_2^z$ with the RKKY-like coupling constants, $J_{e/h}^{RKKY}(\vec{R}_1, \vec{R}_2) = -\frac{1}{4\omega_{e/h}}(\frac{J_{eM/hM}^{2D}}{\pi l_{e/h}^2})^2 (\vec{R}_1 \cdot \vec{R}_2) \exp[-(R_1^2 + R_2^2)/(2l_{e/h}^2)]$, where $l_h = l_e = a_B^* \sqrt{Ry^*/\omega_e}$. The first term in the RKKY interaction comes from the electron scattering and leads to the Heisenberg Mn-Mn interaction. The second term involving the hole scattering leads to an Ising-like Mn-Mn interaction because the heavy-hole spin with $j_z = \pm 3/2$ cannot be flipped by the h-Mn interaction. We find the value of J_h^{RKKY} for typical SADs two orders of magnitude higher than J_e^{RKKY}, with the XX-2Mn energy spectrum dominated by the hole-mediated RKKY interaction. The effective Mn-Mn interaction for even exciton numbers is determined by the relative position of the two Mn's in SADs, and can be either ferromagnetic or anti-ferromagnetic.

We have now shown that Mn-Mn interactions are different depending on the number of excitons in the quantum dot. The odd-even effects presented here can be related to the odd-even effects for electron-mediated interactions in magnetic quantum dots predicted in ref. [28]. Here we further reveal that, via the RKKY interaction mediated by exciton carriers, QDs with even number of excitons exhibit distinctive magnetic phases, depending on Mn ions' spatial configurations. We will show below that the the rich optical patterns corresponding to the magnetic phases are identifiable in the studies of the temperature- and power-dependent emission spectra. Let us now discuss how one can detect the magnetic states of Mn ions from the emission spectra.

In principle, emission spectra depend on the excitation power and energy, as well as on the relaxation mechanism,

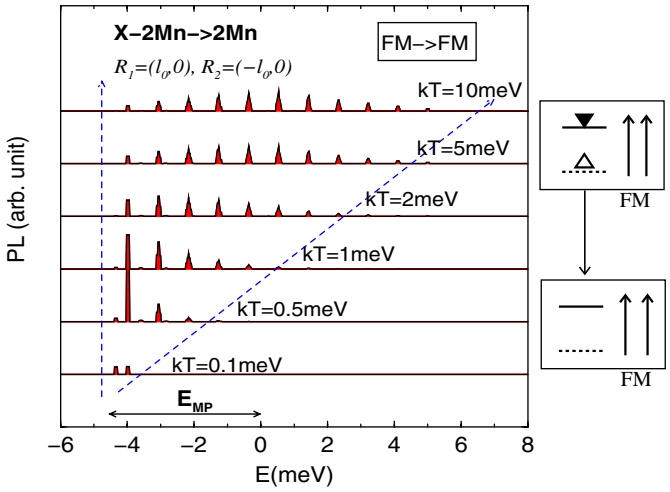

Fig. 2: Emission spectrum of the exciton coupled to two Mn ions as a function of temperature. Transition from dark to bright excitons and magneto-polaron shift are indicated.

which determine both the effective temperature and average exciton population. Here we assume that the quantum dot and Mn ion system reached quasi-equilibrium characterised by common temperature and chemical potential.

In quasi-equilibrium the emission spectrum $A(\omega)$ as a function of photon energy ω due to recombination of excitons coupled to Mn ions is calculated by using Fermi's golden rule: $A(\omega)=\sum_{N_x} F(N_x)\sum_{f,i} F(E_i)|\langle N_x-1, N_{Mn}; f|P^-|N_x, N_{Mn}; i\rangle|^2\delta(\omega-E_i+E_f)$, where $P^-\equiv\sum_{l,\sigma} h_{l-\sigma}c_{l\sigma}$ is the polarization operator, $F(E_i)=\exp(-E_i/k_BT)/[\sum_l \exp(-E_l/k_BT)]$ is the occupation probability of state $|i\rangle$, k_B is the Boltzmann constant, T is temperature, and $F(N_x)$ is the probability of a dot being populated by N_x excitons. The polarization operator P^- couples the N_x-exciton GSs to (N_x-1)-exciton states but does not change the spin of Mn ions.

The emission spectra presented below are calculated for II–VI QDs with $m_e=0.106m_0$, $m_h=0.424m_0$, $\omega_e=4Ry^*$, $\omega_h=Ry^*$, $l_{e/h}\equiv l_0=2.65\,\mathrm{nm}$, where $Ry^*=12.8\,\mathrm{meV}$, $a_B^*=5.29\,\mathrm{nm}$ are the effective Rydberg and the effective Bohr radius for the electron, respectively. The electron-Mn interaction strength is denoted by $J_{eM}^{2D}=J_{eM}^{(0)}2/d$, where $J_{eM}^{(0)}=15\,\mathrm{meV}\cdot\mathrm{nm}^3$ is the coupling constant of the e-Mn exchange interaction and $d=2\,\mathrm{nm}$ the thickness of SAD [21]. The h-Mn coupling is four times higher at $J_{hM}^{(0)}=60\,\mathrm{meV}\cdot\mathrm{nm}^3$. The e-h exchange splitting is taken as $\Delta_0=1.0\,\mathrm{meV}$.

In quasi-equilibrium the emission spectrum is a superposition of emission spectra from different exciton complexes with different weights. Since the weights vary from dot to dot and excitation power and energy, in what follows we present spectra for a specific exciton number.

Figure 2 shows the calculated emission spectra from a single exciton coupled to two Mn ions at positions $R_1=(l_0,0)$ and $R_2=(-l_0,0)$ for different temperatures. At high temperatures, with k_BT comparable to the energy range of the entire bright X-2Mn spectrum ($k_BT>5\,\mathrm{meV}$), and with $J_{eM/hM}(\vec{R}_1)\approx J_{eM/hM}(\vec{R}_2)$, carriers equally access all the 11 X-2Mn shells with all M_z, and we see the corresponding 11 emission lines in fig. 2. As temperature is lowered, carriers occupy only the few low-lying X-2Mn states. The highest-intensity emission line in the low temperature, $kT=0.5\,\mathrm{meV}$ spectrum, comes from the bright exciton coupled to the two Mn ions with parallel spins $M_z=+5$. The lower-intensity line at even lower energy comes from the dark X. The intensity of this line grows as the temperature is lowered. The negative energies of the emission line indicate the lowering of energy of the complex, or the formation of the excitonic magnetic polaron (EMP).

Let us now turn to the emission from the XX complex and discuss the role of the RKKY interaction in the initial state. When the two Mn ions are at $R_1=(l_0,0)$ and $R_2=(-l_0,0)$, we find the RKKY coupling to be anti-ferromagnetic. Figure 3(a) shows the emission spectrum as a function of temperature without the RKKY coupling, and fig. 3(b) shows the emission spectra with the RKKY coupling. Without the RKKY interaction, all states of a spin-singlet XX combined with the two noninteracting Mn's are the initial states in the recombination process. Hence, the XX emission spectrum probes the one exciton final-state spectrum, *i.e.* the spectrum composed of 11 lines, as shown in fig. 2. When the RKKY interaction is taken into account, the Mn complex is anti-ferromagnetic with zero total spin. Hence the emission spectrum selectively maps out the final exciton coupled to Mn ions states with total $M_z=0$, instead of the EMP states. Thus, we see only one main emission line in fig. 3(b), instead of the 11 lines shown in fig. 3(a) for $k_BT\to 0$. The line corresponds to $M_z=0$ states and is located in the middle of the spectrum.

Let us now change the position of magnetic ions to $\vec{R}_1=(l_0,0)$ and $\vec{R}_2=\frac{1}{\sqrt{2}}(l_0,l_0)$. With the XX present, this leads to ferromagnetically coupled Mn ions. Figure 3(c) shows the XX emission spectra. At low temperature, $k_BT<0.05\,\mathrm{meV}$, the emission spectrum contains two well-separated lines instead of one, shown in fig. 3(c). The two lines in fig. 3(c) correspond to the two bright EMP exciton states, corresponding to two aligned Mn spins pointing in two opposite directions. The energy difference is the EMP Zeeman energy. Clearly, the optical spectra distinguish between the ferromagnetic and anti-ferromagnetic state of Mn ions. Hence one can identify the magnetic properties of the multi-Mn complex by controlling the exciton number and measuring the low-temperature emission spectra.

In summary, we present a theory of the control of magnetic properties of magnetic ions via the optical control of the average population of photo-excited electrons and holes. We show that odd exciton complexes couple directly to spins of Mn ions via the *sp-d* exchange interaction and form excitonic magnetic polarons. The

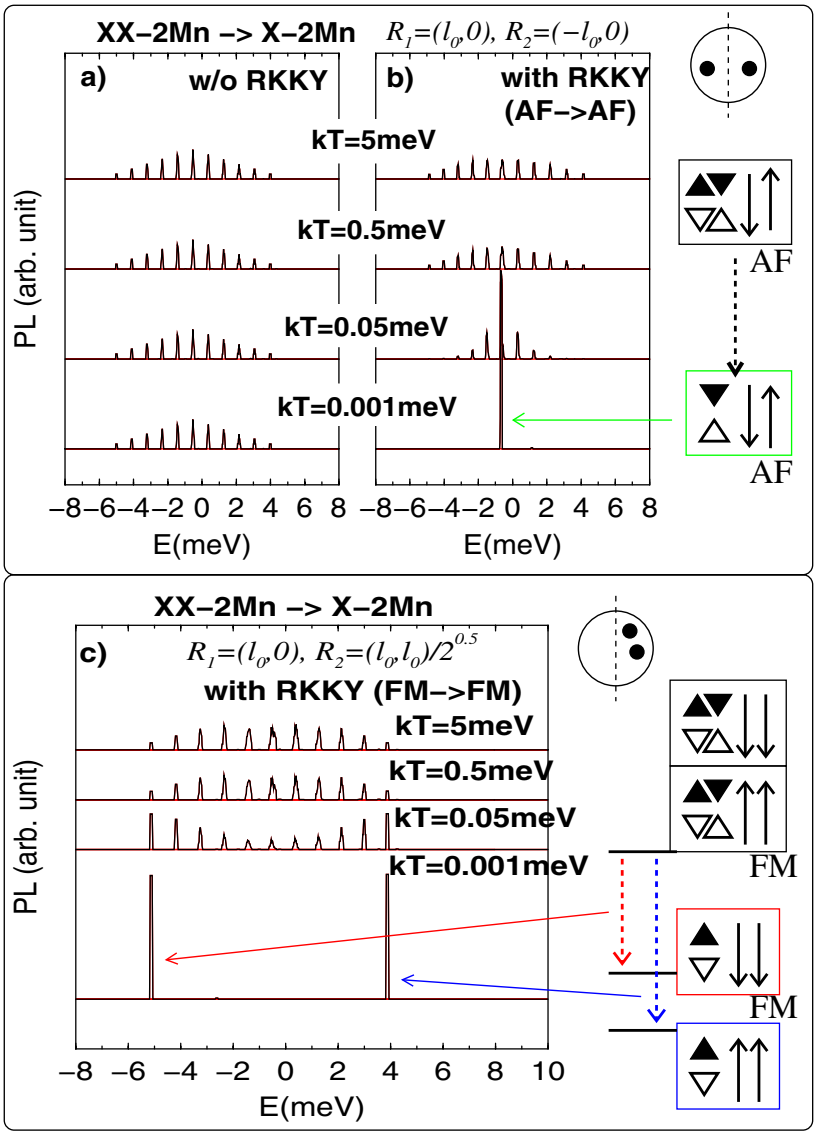

Fig. 3: Emission spectrum of the bi-exciton to exciton-magneto-polaron final-state complex as a function of temperature (a) without the RKKY interaction, and (b) including the anti-ferromagnetic (AF) RKKY interaction among the two Mn ions. (c) Detection of the exciton-magneto-polaron giant Zeeman splitting in the emission spectrum from the bi-exciton coupled to 2 Mn ions to an exciton-magneto-polaron final-state complex as a function of temperature with the RKKY ferromagnetic (FM) interaction in the initial state.

even exciton numbers generate a long-ranged RKKY Mn-Mn interaction leading to either ferromagnetism or anti-ferromagnetism of exciton-coupled Mn ions. The signatures of excitonic magnetic polarons and magnetic state of Mn ions in emission spectra as a function of the number of excitons are predicted.

* * *

S-JC acknowledges the National Science Council of Taiwan for financial support under Contract No. NSC-95-2112-M-009-033-MY3 and the Institute for Microstructural Sciences for hospitality. PH acknowledges discussions with J. Kossut and partial support by the Canadian Institute for Advanced Research and by Quantum Works.

REFERENCES

[1] Awschalom D. D., Loss D. and Samarth N., *Semiconductor Spintronics and Quantum Computation Series on Nanoscience and Technology* (Springer-Verlag, Berlin) 2002.
[2] Furdyna J. K., *J. Appl. Phys.*, **64** (1988) R29.
[3] Žutić I., Fabian J. and Das Sarma S., *Rev. Mod. Phys.*, **76** (2004) 323.
[4] Ohno H., Chiba D., Matsukura F., Omiya T., Abe E., Dietl T., Ohno Y. and Ohtani K., *Nature (London)*, **408** (2000) 944; Chiba D., Yamanouchi M., Matsukura F. and Ohno H., *Science*, **301** (2003) 943.
[5] Yamanouchi M., Chiba D., Matsukura F. and Ohno H., *Nature*, **428** (2004) 539.

[6] Kato Y., Myers R. C., Gossard A. C. and Awschalom D. D., *Nature*, **427** (2004) 50.

[7] Kimel A. V., Kirilyuk A., Usachev P. A., Pisarev R. V., Balbashov A. M. and Rasing Th., *Nature*, **435** (2005) 655.

[8] Oiwa A., Mitsumori Y., Moriya R., Slupinski T. and Munekata H., *Phys. Rev. Lett.*, **88** (2002) 137202.

[9] Lottermoser T., Lonkai T., Amann U., Hohlwein D., Ihringer J. and Fiebig M., *Nature*, **430** (2004) 541.

[10] Hawrylak P. and Korkusinski M., *Single Quantum dots: Fundamentals Applications, and New Concepts, Topics Appl. Phys.*, edited by Michler P., Vol. **90** (Springer-Verlag, Berlin) 2003.

[11] Gould C., Slobodskyy A., Supp D., Slobodskyy T., Grabs P., Hawrylak P., Qu F., Schmidt G. and Molenkamp L. W., *Phys. Rev. Lett.*, **97** (2006) 017202.

[12] Efros A. L., Rosen M. and Rashba E. I., *Phys. Rev. Lett.*, **87** (2001) 206601.

[13] Govorov A. O., *Phys. Rev. B*, **72** (2005) 075359.

[14] Léger Y., Besombes L., Fernandez-Rossier J., Maingault L. and Mariette H., *Phys. Rev. Lett.*, **95** (2005) 047403.

[15] Climente J. I., Korkusinski M., Hawrylak P. and Planelles J., *Phys. Rev. B*, **71** (2005) 125321.

[16] Abolfath R. M., Hawrylak P. and Žutić I., *Phys. Rev. Lett.*, **98** (2007) 207203.

[17] Bhattacharjee A. K. and Benoit á la Guillaume C., *Phys. Rev. B*, **55** (1997) 10613.

[18] Liu W. K., Whitaker K. M., Kittilstved K. R. and Gamelin D. R., *J. Am. Chem. Soc.*, **126** (2006) 3910.

[19] Hoffman D. M., Meyer B. K., Ekimov A. I., Merkulov I. A., Efros A. L., Rosen M., Couino G., Gacoin T. and Boilot J. P., *Solid State Commun.*, **114** (2000) 547.

[20] Fernandez-Rossier J. and Aguado R., *Phys. Rev. Lett.*, **98** (2007) 106805.

[21] Qu F. and Hawrylak P., *Phys. Rev. Lett.*, **96** (2006) 157201.

[22] Mackowski S., Gurung T., Nguyen A., Jackson H. E., Smith L. M., Karczewski G. and Kossut J., *Appl. Phys. Lett.*, **84** (2004) 3337.

[23] Seufert J., Bacher G., Scheibner M., Forchel A., Lee S., Dobrowolska M. and Furdyna J. K., *Phys. Rev. Lett.*, **88** (2002) 027402.

[24] Wojnar P., Suffczyński J., Kowalik K., Golnik A., Karczewski G. and Kossut J., *Phys. Rev. B*, **75** (2007) 155301.

[25] Hundt A., Puls J. and Henneberger F., *Phys. Rev. B*, **69** (2004) 121309(R).

[26] Bayer M., Stern O., Hawrylak P., Fafrad S. and Forchel A., *Nature*, **405** (2000) 923.

[27] Sheng W., Cheng S. J. and Hawrylak P., *Phys. Rev. B*, **71** (2005) 035316.

[28] Fernandez-Rossier J. and Brey L., *Phys. Rev. Lett.*, **93** (2004) 117201.

[29] Piermarocchi C., Chen P., Dale Y. S. and Sham L. J., *Phys. Rev. B*, **65** (2002) 075307.

[30] Piermarocchi C., Chen P., Sham L. J. and Steel D. G., *Phys. Rev. Lett.*, **89** (2002) 167402.

[31] Besombes L., Léger Y., Maingault L., Ferrand D., Mariette H. and Cibert J., *Phys. Rev. Lett.*, **93** (2004) 207403.

[32] Besombes L., Léger Y., Maingault L., Ferrand D., Mariette H. and Cibert J., *Phys. Rev. B*, **71** (2005) 161307.

[33] Govorov A. O., *Phys. Rev. B*, **70** (2004) 035321.

[34] Fernandez-Rossier J., *Phys. Rev. B*, **73** (2006) 045301.

[35] Hawrylak P., *Phys. Rev. Lett.*, **71** (1993) 3347.

[36] Raymond S., Studenikin S., Sachrajda A., Wasilewski Z., Cheng S. J., Sheng W., Hawrylak P., Babinski A., Potemski M., Ortner G. and Bayer M., *Phys. Rev. Lett.*, **92** (2004) 187402.

[37] Sheng W. and Hawrylak P., *Phys. Rev. B*, **73** (2006) 125331.

[38] Bayer M., Ortner G., Stern O., Kuther A., Gorbunov A. A., Forchel A., Hawrylak P., Fafard S., Hinzer K., Reinecke T. L., Walck S. N., Reithmaier J. P., Klopf F. and Schäfer F., *Phys. Rev. B*, **65** (2002) 195315.